

Article

# Electrosynthesis of Copolymers Based on 1,3,5-Tris(*N*-Carbazolyl)Benzene and 2,2'-Bithiophene and Their Applications in Electrochromic Devices

Chung-Wen Kuo \* and Po-Ying Lee

Department of Chemical and Materials Engineering, National Kaohsiung University of Applied Sciences, Kaohsiung 80778, Taiwan; k40017105@gcloud.csu.edu.tw

\* Correspondence: welly@cc.kuas.edu.tw; Tel.: +886-7-381-4526 (ext. 5138)

Received: 12 September 2017; Accepted: 13 October 2017; Published: 17 October 2017

**Abstract:** Poly(1,3,5-tris(*N*-carbazolyl)benzene) (PtnCz) and three copolymers based on 1,3,5-tris(*N*-carbazolyl)benzene (tnCz) and 2,2'-bithiophene (bTp) were electrochemically synthesized. The anodic P(tnCz1-bTp2) film with a tnCz/bTp feed molar ratio of 1/2 showed four colors (light orange at 0.0 V, yellowish-orange at 0.7 V, yellowish-green at 0.8 V, and blue at 1.1 V) from the neutral state to oxidized states. The optical contrast ( $\Delta T\%$ ) and coloration efficiency ( $\eta$ ) of the P(tnCz1-bTp2) film were measured as 48% and  $112 \text{ cm}^2 \cdot \text{C}^{-1}$ , respectively, at 696 nm. Electrochromic devices (ECDs) based on PtnCz, P(tnCz1-bTp1), P(tnCz1-bTp2), P(tnCz1-bTp4), and PbTp films as anodic polymer layers and poly(3,4-dihydro-3,3-dimethyl-2H-thieno[3,4-b-1,4]dioxepin) (PProDOT-Me<sub>2</sub>) as cathodic polymer layers were assembled. P(tnCz1-bTp2)/PProDOT-Me<sub>2</sub> ECD showed three various colors (saffron yellow, yellowish-blue, and dark blue) at potentials ranging from  $-0.3$  to 1.5 V. In addition, P(tnCz1-bTp2)/PProDOT-Me<sub>2</sub> ECD showed a high  $\Delta T\%$  value (40% at 630 nm) and a high coloration efficiency ( $519 \text{ cm}^2 \cdot \text{C}^{-1}$  at 630 nm).

**Keywords:** conjugated polymer; polycarbazole; electrochromic device; electrosynthesis; optical contrast; coloration efficiency

## 1. Introduction

Organic redox-active materials have attracted great interest during the past decades for their potential applications in commercial electronic devices [1–3].  $\pi$ -Conjugated polymers (CPs) have been recognized as an important class of organic redox-active materials. Recently, scientists have paid attention to the applications of CPs as electrode materials in electrochromic devices (ECDs) because CPs are capable of changing their optical properties at various voltages [4]. CPs have been extensively used for several regions, such as solar cells [5,6], catalysts [7–9], polymer light-emitting diodes [10–12], supercapacitors [13,14], sensors [15,16], and ECDs [17,18].

The most widely used CPs for electrochromic applications are polyanilines (PANIs) [19], polythiophenes (PThs) [20], polypyrroles (PPys) [21], poly(3,4-ethylenedioxythiophene)s (PEDOTs) [22–24], polycarbazoles (PCzs) [25], and polyindoles [26]. Thin films of these CPs were prepared using chemical synthesis or electrodeposition. PCzs have been widely investigated because of their attractive and practical opto-electrochemical properties. Carbazole units can be substituted or attached at the 3,6-, 2,7- and *N*-positions; a broad variety of aryl groups can be incorporated at the 3,6-, 2,7- and *N*-positions of carbazole units, and the opto-electronic properties of PCzs can be effectively tuned by incorporating the substituted group at various positions of PCzs [27–29]. PThs are one of the most precious types of CPs that may be easily modified to offer a variety of useful physicochemical and electrochemical properties [30]. PThs without other substituents are insoluble in any solvent; PEDOTs and poly(3,4-dihydro-3,3-dimethyl-2H-thieno[3,4-b-1,4]dioxepin) (PProDOT-Me<sub>2</sub>) contain

two electron-donating oxygen atoms at the 3,4-positions of Th unit, which shows a higher solubility than that of PTh. Moreover, the band gaps of PEDOTs and PProDOT-Me<sub>2</sub> are lower than that of PTh, and PEDOTs as an EC material have showed promising properties in electrochromic iris devices [22]. On the other hand, the copolymerization of specific monomers can bring about more interesting electrochemical and electrochromic properties than that of homopolymers. Accordingly, three copolymers based on 1,3,5-tris(*N*-carbazolyl)benzene (tnCz) and 2,2'-bithiophene (bTp) and two homopolymers (poly(1,3,5-tris(*N*-carbazolyl)benzene) and poly(2,2'-bithiophene)) were synthesized electrochemically in this study. 1,3,5-Tris(*N*-carbazolyl)benzene contains three carbazole units linked by a phenyl unit, which offers several polymerization locations at the 3,6-positions of three carbazole units. The electrochromic and spectroelectrochemical properties of two homopolymer films and three copolymer films were comprehensively studied. Moreover, five ECDs were fabricated using PtnCz, P(tnCz1-bTp1), P(tnCz1-bTp2), P(tnCz1-bTp4), and PbTp films as the anodic layers, and PProDOT-Me<sub>2</sub> as the cathodic layer. The spectroelectrochemical characterization, coloration efficiency, switching time, and multiple cycling stability of PtnCz/PProDOT-Me<sub>2</sub>, P(tnCz1-bTp1)/PProDOT-Me<sub>2</sub>, P(tnCz1-bTp2)/PProDOT-Me<sub>2</sub>, P(tnCz1-bTp4)/PProDOT-Me<sub>2</sub>, and PbTp/PProDOT-Me<sub>2</sub> ECDs were also studied.

## 2. Materials and Methods

### 2.1. Materials

ProDOT-Me<sub>2</sub> was synthesized on the basis of previously published procedures [31]; bTp, tris(4-iodophenyl)amine, and LiClO<sub>4</sub> were purchased from Sigma-Aldrich (St. Louis, MO, USA). Poly(methyl methacrylate) (PMMA) (*M*<sub>w</sub> = 350,000), 18-crown-6, and carbazole were purchased from Acros Organics (Geel, Belgium). Acetonitrile (ACN) was purchased from Alfa Aesar (Haverhill, MA, USA) and was used as received.

### 2.2. Synthesis of 1,3,5-Tris(*N*-Carbazolyl)Benzene (tnCz)

A mixture of 1,3,5-tribromobenzene (69.26 mg, 0.22 mmol), carbazole (140.45 mg, 0.84 mmol), potassium carbonate (331.7 mg, 2.4 mmol), 18-crown-6 (17.44 mg, 0.066 mmol), copper bronze (139.17 mg, 2.19 mmol) and 70 mL of 1,2-dichlorobenzene was stirred under nitrogen for 36 h at 185 °C. Afterwards, 1,2-dichlorobenzene was evaporated and the remaining mixture was purified by column chromatography (silica gel; 1:2 dichloromethane (DCM)/hexane) to give 1,3,5-tris(*N*-carbazolyl)benzene with a yield of 46%. <sup>1</sup>H NMR (500 MHz, dimethyl sulfoxide (DMSO)-d<sub>6</sub>): δ of 8.28 (d, 6H, Cz-H), 8.05 (s, 3H, phenyl-H), 7.77 (d, 6H, Cz-H), 7.52 (dd, 6H, Cz-H), and 7.34 (dd, 6H, Cz-H). Elem. anal. calcd. for C<sub>42</sub>H<sub>27</sub>N<sub>3</sub>: C, 87.93%; H, 4.74%; N, 7.32%. Found: C, 87.78%; H, 4.69%; N, 7.21%.

### 2.3. Electrochemical Polymerization

Electrochemical polymerizations of PtnCz, P(tnCz1-bTp1), P(tnCz1-bTp2), P(tnCz1-bTp4), and PbTp films were carried out in a three-electrode system. A platinum wire and a Ag/AgCl electrode were used as counter and reference electrodes, respectively. PtnCz, P(tnCz1-bTp1), P(tnCz1-bTp2), P(tnCz1-bTp4), and PbTp films were prepared potentiodynamically at the potential range of 0.0–1.9 V (vs. Ag/AgCl) at 100 mV·s<sup>-1</sup> for three cycles. The feed species of anodic polymer films are listed in Table 1. The active areas of PtnCz, P(tnCz1-bTp1), P(tnCz1-bTp2), P(tnCz1-bTp4), and PbTp films were 1.0 × 1.5 cm<sup>2</sup>.

### 2.4. Construction of Dual-Type ECDs

The electrochromic electrolyte was prepared using a mixture solution of PMMA, LiClO<sub>4</sub>, ACN, and DCM according to our previous procedures [32]. Five anodic layers (PtnCz, P(tnCz1-bTp1), P(tnCz1-bTp2), P(tnCz1-bTp4), and PbTp films) and a PProDOT-Me<sub>2</sub> layer faced each other

to assemble PtnCz/PProDOT-Me<sub>2</sub>, P(tnCz1-bTp1)/PProDOT-Me<sub>2</sub>, P(tnCz1-bTp2)/PProDOT-Me<sub>2</sub>, P(tnCz1-bTp4)/PProDOT-Me<sub>2</sub>, and PbTp/PProDOT-Me<sub>2</sub> ECDs, which were separated by an electrochromic electrolyte. The length and width of the electrochromic devices were 1.5 and 1.0 cm, respectively.

**Table 1.** Feed species of anodic layers (a)–(e).

| Electrodes | Anodic Polymer | Feed Species of Anodic Polymer | Feed Molar Ratio of Anodic Polymer |
|------------|----------------|--------------------------------|------------------------------------|
| (a)        | PtnCz          | 2 mM tnCz                      | Neat tnCz                          |
| (b)        | P(tnCz1-bTp1)  | 2 mM tnCz + 2 mM bTp           | 1:1                                |
| (c)        | P(tnCz1-bTp2)  | 2 mM tnCz + 4 mM bTp           | 1:2                                |
| (d)        | P(tnCz1-bTp4)  | 1 mM tnCz + 4 mM bTp           | 1:4                                |
| (e)        | PbTp           | 4 mM bTp                       | Neat bTp                           |

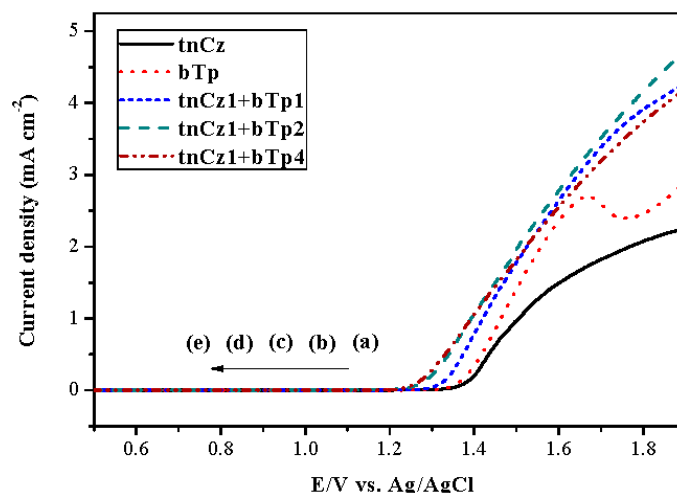
### 2.5. Spectroelectrochemical and Electrochemical Characterization

The electrochemical experiments were characterized using a CHI627D electrochemical analyzer (CH Instruments, Austin, TX, USA). A platinum wire, an Indium Tin Oxide (ITO) glass (1.5 cm<sup>2</sup>), and an Ag/AgCl electrode were employed as the counter electrode, working electrode, and reference electrode, respectively. The spectroelectrochemical measurements were carried out using an Agilent Cary 60 UV–Visible spectrophotometer (Varian Inc., Walnut Creek, CA, USA) to monitor the UV–Visible spectra. Double potential chronoamperometry was performed with the three-electrode cell using an Agilent Cary 60 UV–Visible spectrophotometer and a CHI627D electrochemical analyzer.

## 3. Results and Discussion

### 3.1. Electrochemical Polymerizations

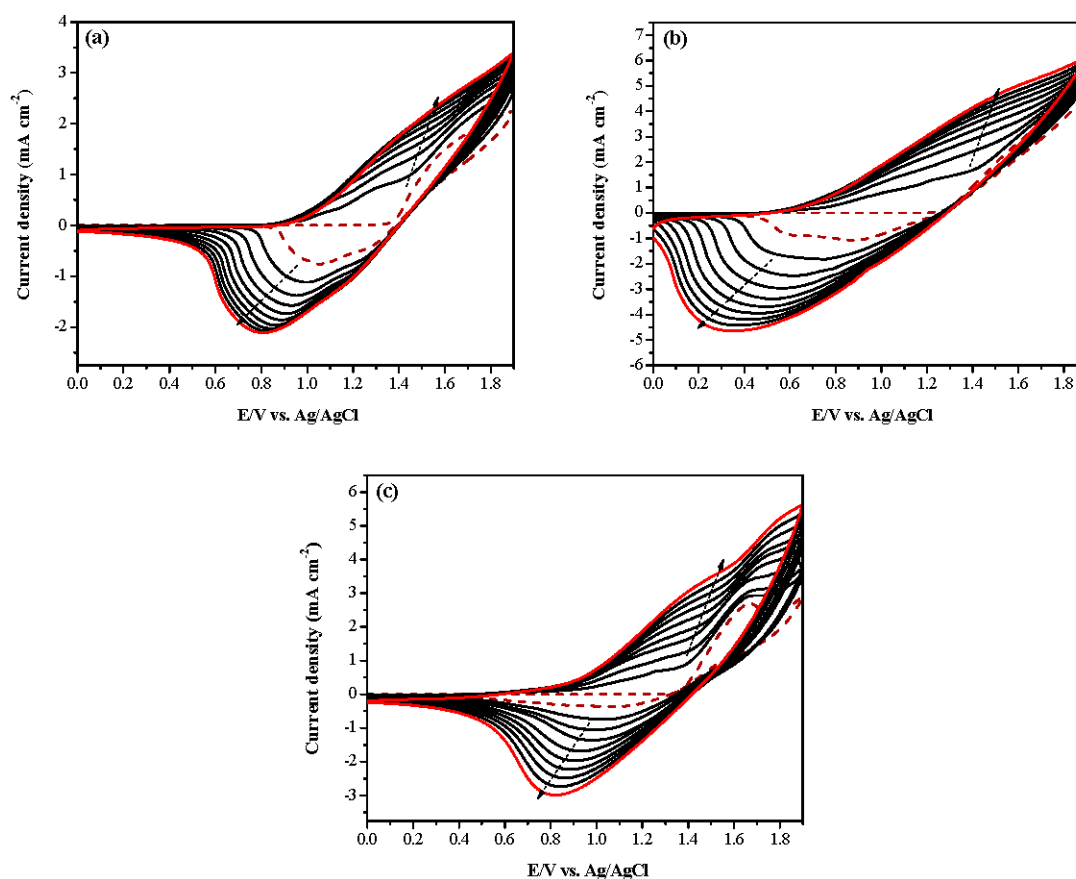
Figure 1 shows the anodic polarization curves of the neat tnCz, the neat bTp, and the mixtures (tnCz + bTp) in ACN/DCM (1:2, by volume) solution containing 0.2 M LiClO<sub>4</sub> at a constant scan rate of 100 mV·s<sup>-1</sup>. The onset voltage of neat tnCz, neat bTp, tnCz1 + bTp1 (tnCz/bTp = 1:1, by feed molar ratio), tnCz1 + bTp2 (tnCz/bTp = 1:2, by feed molar ratio), and tnCz1+bTp4 (tnCz:bTp = 1:4, by feed molar ratio) were 1.36, 1.35, 1.32, 1.26, and 1.25 V, respectively.



**Figure 1.** Anodic polarization curves of (a) 2 mM tnCz, (b) 4 mM bTp, (c) 2 mM tnCz + 2 mM bTp, (d) 2 mM tnCz + 4 mM bTp, and (e) 1 mM tnCz + 4 mM bTp in ACN/DCM (1:2, by volume) containing 0.2 M LiClO<sub>4</sub> at a scan rate of 100 mV·s<sup>-1</sup>.

The  $E_{\text{onset}}$  of PtnCz was comparable to that of PbTp, implying that PtnCz shows a similar electron-donating ability to that of PbTp. However, P(tnCz1-bTp1), P(tnCz1-bTp2) and P(tnCz1-bTp4) showed lower  $E_{\text{onset}}$  values than those of PtnCz and PbTp, indicating that the  $E_{\text{onset}}$  of copolymers is lower than those of homopolymers. The onset potential of neat tnCz was close to that of neat bTp, demonstrating that the copolymerizations of tnCz and bTp are practicable.

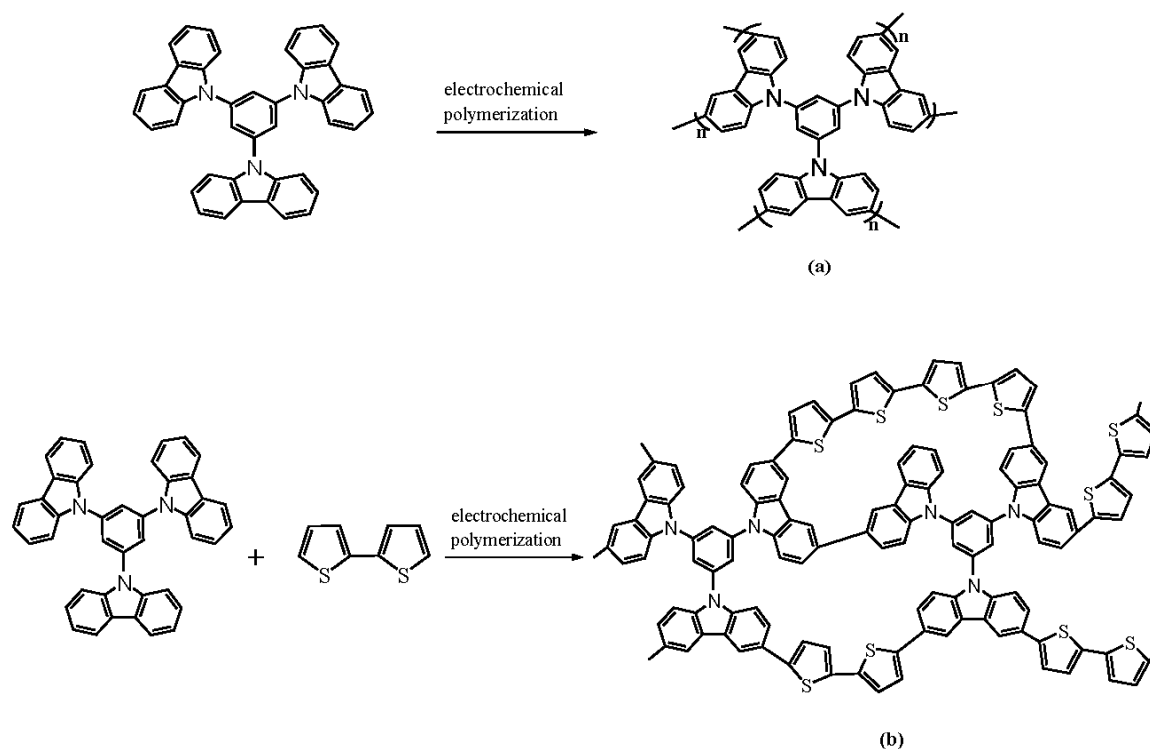
Figure 2a–c shows the electrochemical synthesis of neat tnCz, mixture (tnCz + bTp), and neat bTp in 0.2 M LiClO<sub>4</sub>/(ACN/DCM (1:2, by volume)) solution, respectively. The current density of cyclic voltammetry (CV) curves in Figure 2a–c increases with an increasing number of scanning cycles, implying the growth of PtnCz, P(tnCz1-bTp2), and PbTp on the ITO electrode [21]. As displayed in Figure 2a, the oxidation and reduction peaks of PtnCz, located at 1.31 and 0.98 V, respectively, are smaller than those of PbTp (the oxidation and reduction peaks of PbTp are situated at 1.68 and 1.04 V, respectively). The redox peaks of the P(tnCz1-bTp2) film shifted to lower potentials than those of PtnCz and PbTp, indicating that the copolymer gives rise to lower redox peaks than those of homopolymers. Moreover, the locations of the oxidation and reduction peaks and the waveshapes of the CV curves of the P(tnCz1-bTp2) film are different to those of the PtnCz and PbTp films, demonstrating the formation of the P(tnCz1-bTp2) film.



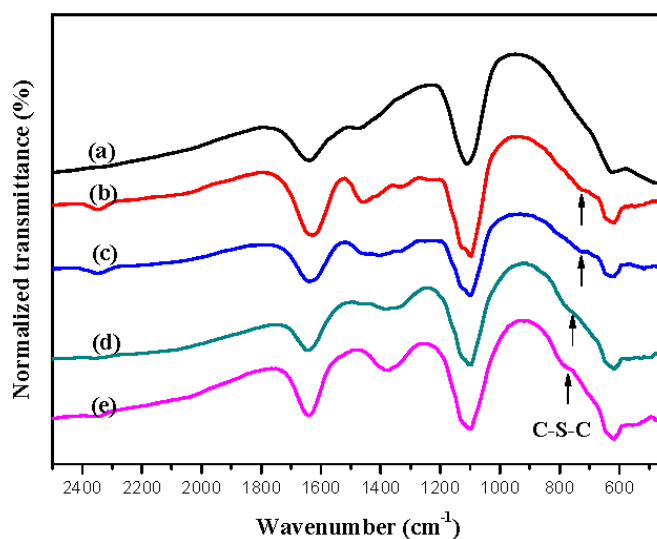
**Figure 2.** Electrochemical polymerizations of (a) PtnCz, (b) P(tnCz1-bTp2), and (c) PbTp in ACN/DCM (1:2, by volume) solution at 100 mV·s<sup>-1</sup> on ITO working electrode.

The electrochemical polymerization routes of PtnCz and P(tnCz1-bTp2) are shown in Figure 3. Moreover, the homopolymers (PtnCz and PbTp) and copolymers (P(tnCz1-bTp1), P(tnCz1-bTp2), and P(tnCz1-bTp4)) were further studied using Fourier transform infrared (FT-IR). As shown in Figure 4, the C–S–C characteristic peaks of the P(tnCz1-bTp1), P(tnCz1-bTp2), P(tnCz1-bTp4), and PbTp films, located at 730, 735, 760, and 783 cm<sup>-1</sup>, and the C–S–C characteristic peaks of P(tnCz1-bTp1),

P(tnCz1-bTp2), and P(tnCz1-bTp4) are different to those of PbTp, indicating that copolymerization occurs during the electrochemical polymerization of PtnCz and PbTp.

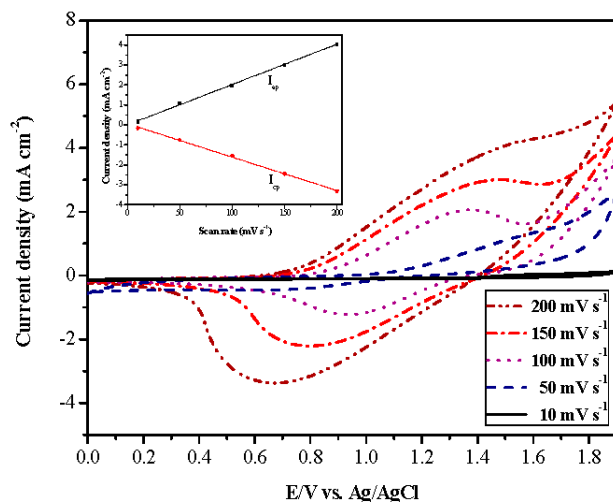


**Figure 3.** The electrochemical polymerization routes of (a) PtnCz and (b) P(tnCz1-bTp2).



**Figure 4.** FT-IR spectra of (a) PtnCz, (b) P(tnCz1-bTp1), (c) P(tnCz1-bTp2), (d) P(tnCz1-bTp4), and (e) PbTp.

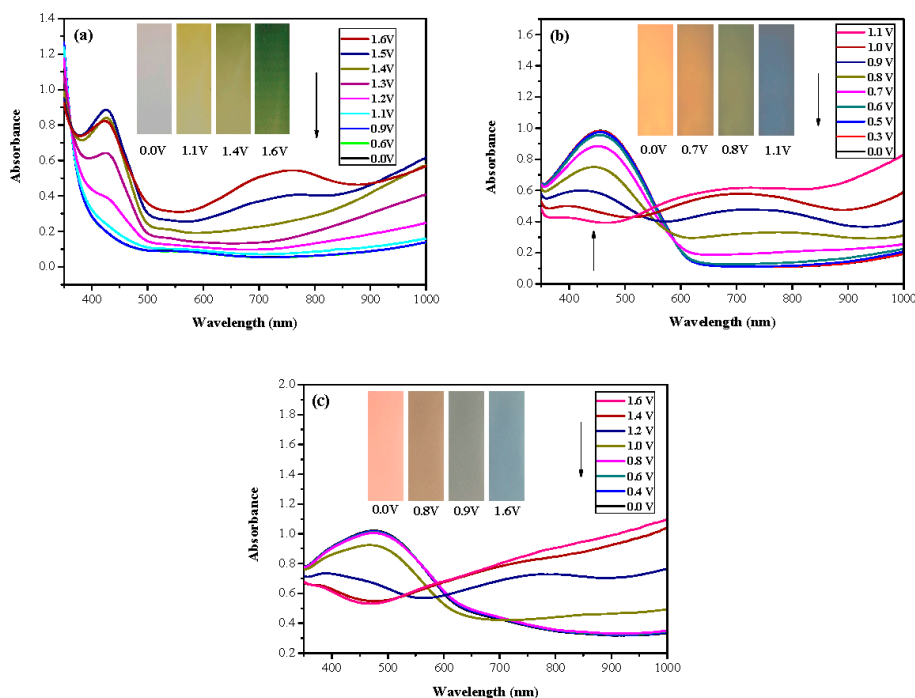
The as-prepared P(tnCz1-bTp2) film was also investigated at several scan rates between 10 and 200  $\text{mV}\cdot\text{s}^{-1}$  in  $\text{LiClO}_4/(\text{ACN} + \text{DCM})$  solution. As displayed in Figure 5, the P(tnCz1-bTp2) film showed distinct redox peaks, and the current density of the reduction and oxidation peaks showed a linear relationship with the scan rate, indicating that the P(tnCz1-bTp2) film was well-adhered onto indium tin oxide conductive glass and that the reduction and oxidation processes of P(tnCz1-bTp2) film were nondiffusional processes [33].



**Figure 5.** CV curves of the P(tnCz1-bTp2) film at several scan rates between 10 and 200  $\text{mV}\cdot\text{s}^{-1}$  in the  $\text{LiClO}_4 + \text{ACN} + \text{DCM}$  solution. Scan rate dependence of the P(tnCz1-bTp2) anodic and cathodic peak current densities, respectively (inset).

### 3.2. Spectroelectrochemical Characterizations of PtnCz, P(tnCz-bTp), and PbTp Films

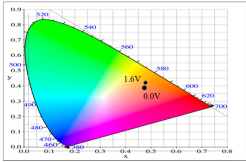
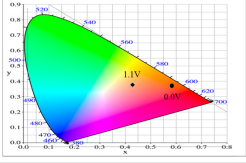
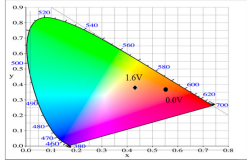
Spectroelectrochemical characterizations of the PtnCz, P(tnCz1-bTp1), P(tnCz1-bTp2), P(tnCz1-bTp4), and PbTp films were carried out in 0.2 M  $\text{LiClO}_4 / (\text{ACN} + \text{DCM})$  solution. Figure 6a–c shows the UV–Vis spectra of the PtnCz, P(tnCz1-bTp2), and PbTp films, respectively, at various potentials. As shown in Figure 6a, the PtnCz film does not show a distinct absorption peak in its neutral state. Nevertheless, new absorption bands appear at 430 and 750 nm after a potential of more than 1.2 V was applied, which can be ascribed to the generation of polaron and bipolaron bands for the PtnCz film [34].



**Figure 6.** UV–Visible spectra of (a) PtnCz, (b) P(tnCz1-bTp2), and (c) PbTp electrodes on ITO in an ACN + DCM solution containing 0.2 M  $\text{LiClO}_4$ .

The P(tnCz1-bTp2) and PbTp films show  $\pi$ - $\pi^*$  transition peaks of thiophene chains at 450 and 480 nm, respectively, in their neutral state, and the P(tnCz1-bTp2) and PbTp films show polaron and bipolaron bands at 700 and 900 nm, respectively. The PtnCz film in 0.2 M LiClO<sub>4</sub>/(ACN + DCM) solution was light grey in the neutral state (0.0 V), yellow in the intermediate state (1.1 V), yellowish-green in the oxidized state (1.4 V), and green in highly oxidized states (1.6 V). For the copolymer films in 0.2 M LiClO<sub>4</sub>/(ACN + DCM) solution, the P(tnCz1-bTp2) film was light orange in the neutral state (0.0 V), yellowish-orange (0.7 V) and yellowish-green (0.8 V) in the intermediate state, and blue in oxidized states (1.1 V). The P(tnCz1-bTp2) film exhibited different colors to PtnCz film in the oxidized states. Under similar conditions, the PbTp film in 0.2 M LiClO<sub>4</sub>/(ACN + DCM) solution was tangerine in the neutral state (0.0 V), yellowish-brown in the intermediate state (0.8 V), cadet blue in the oxidized state (0.9 V), and blue in highly oxidized states (1.6 V). The colorimetric parameters of the PtnCz, P(tnCz1-bTp2), and PbTp films in 0.2 M LiClO<sub>4</sub>/(ACN + DCM) solution are shown in Table 2.

**Table 2.** Colorimetric values ( $L^*$ ,  $a^*$ , and  $b^*$ ), CIE (Commission Internationale de l'Éclairage) chromaticity values ( $x$ ,  $y$ ) and diagrams of the PtnCz, P(tnCz1-bTp2), and PbTp films at various applied potentials.

| Polymers      | Potential (V) | $L^*$ | $a^*$ | $b^*$  | $x$    | $y$    | Diagrams                                                                              |
|---------------|---------------|-------|-------|--------|--------|--------|---------------------------------------------------------------------------------------|
| PtnCz         | 0.0           | 92.77 | 1.22  | 7.05   | 0.4567 | 0.4125 |   |
|               | 1.1           | 91.69 | 0.96  | 9.62   | 0.4589 | 0.4152 |                                                                                       |
|               | 1.2           | 89.86 | 0.48  | 19.25  | 0.4676 | 0.4243 |                                                                                       |
|               | 1.3           | 87.25 | 0.00  | 31.83  | 0.4785 | 0.4356 |                                                                                       |
|               | 1.4           | 83.10 | -1.91 | 36.46  | 0.4802 | 0.4431 |                                                                                       |
|               | 1.5           | 78.08 | -5.35 | 33.74  | 0.4728 | 0.4480 |                                                                                       |
|               | 1.6           | 73.61 | -7.75 | 25.77  | 0.4616 | 0.4465 |                                                                                       |
| P(tnCz1-bTp2) | 0.0           | 71.78 | 34.58 | 54.01  | 0.5661 | 0.3964 |  |
|               | 0.6           | 72.11 | 32.68 | 52.59  | 0.5614 | 0.3989 |                                                                                       |
|               | 0.7           | 72.03 | 25.51 | 47.02  | 0.5445 | 0.4078 |                                                                                       |
|               | 0.8           | 70.79 | 12.38 | 33.90  | 0.5098 | 0.4209 |                                                                                       |
|               | 0.9           | 67.83 | -1.02 | 14.63  | 0.4640 | 0.4260 |                                                                                       |
|               | 1.0           | 64.23 | -7.63 | -2.57  | 0.4274 | 0.4161 |                                                                                       |
|               | 1.1           | 62.30 | -7.98 | -12.05 | 0.4119 | 0.4029 |                                                                                       |
| PbTp          | 0.0           | 51.45 | 21.71 | 23.34  | 0.5357 | 0.3929 |  |
|               | 0.6           | 51.01 | 20.62 | 21.90  | 0.5318 | 0.3936 |                                                                                       |
|               | 0.8           | 51.01 | 20.34 | 21.58  | 0.5307 | 0.3939 |                                                                                       |
|               | 0.9           | 55.79 | 19.12 | 24.19  | 0.5229 | 0.4000 |                                                                                       |
|               | 1.2           | 57.79 | -2.40 | 8.42   | 0.4543 | 0.4231 |                                                                                       |
|               | 1.4           | 55.13 | -7.32 | -7.38  | 0.4177 | 0.4089 |                                                                                       |
|               | 1.6           | 54.83 | -7.08 | -9.69  | 0.4143 | 0.4047 |                                                                                       |

The electrochromic switching of the PtnCz, P(tnCz1-bTp2), and PbTp films was examined using double-potential-step chronoamperometry [35]. Figure 7 shows the transmittance–time profiles of the PtnCz, P(tnCz1-bTp2), and PbTp films in 0.2 M LiClO<sub>4</sub>/(ACN + DCM) solution with a residence time of 10 s;  $\Delta T$ , the optical density ( $\Delta OD$ ), and the coloration efficiency ( $\eta$ ) of the PtnCz, P(tnCz1-bTp1), P(tnCz1-bTp2), P(tnCz1-bTp4), and PbTp films in 0.2 M LiClO<sub>4</sub>/(ACN + DCM) solution are shown in Table 3. The  $\Delta T$  value of the PtnCz, P(tnCz1-bTp1), P(tnCz1-bTp2), P(tnCz1-bTp4), and PbTp films were 28.6%, 45.0%, 48.0%, 36.7%, and 28.1%, respectively. The copolymers (P(tnCz1-bTp1), P(tnCz1-bTp2), and P(tnCz1-bTp4)) showed higher  $\Delta T$  values than the homopolymers (PtnCz and PbTp) in 0.2 M LiClO<sub>4</sub>/(ACN + DCM) solution, implying that the copolymerization of tnCZ with the bTp monomer leads to an increase in the  $\Delta T_{\max}$  value in 0.2 M LiClO<sub>4</sub>/(ACN + DCM) solution. The P(tnCz1-bTp2) film showed the highest  $\Delta T$  value (48%) at 696 nm among these polymer films.

$\Delta OD$  can be estimated by the following equation:

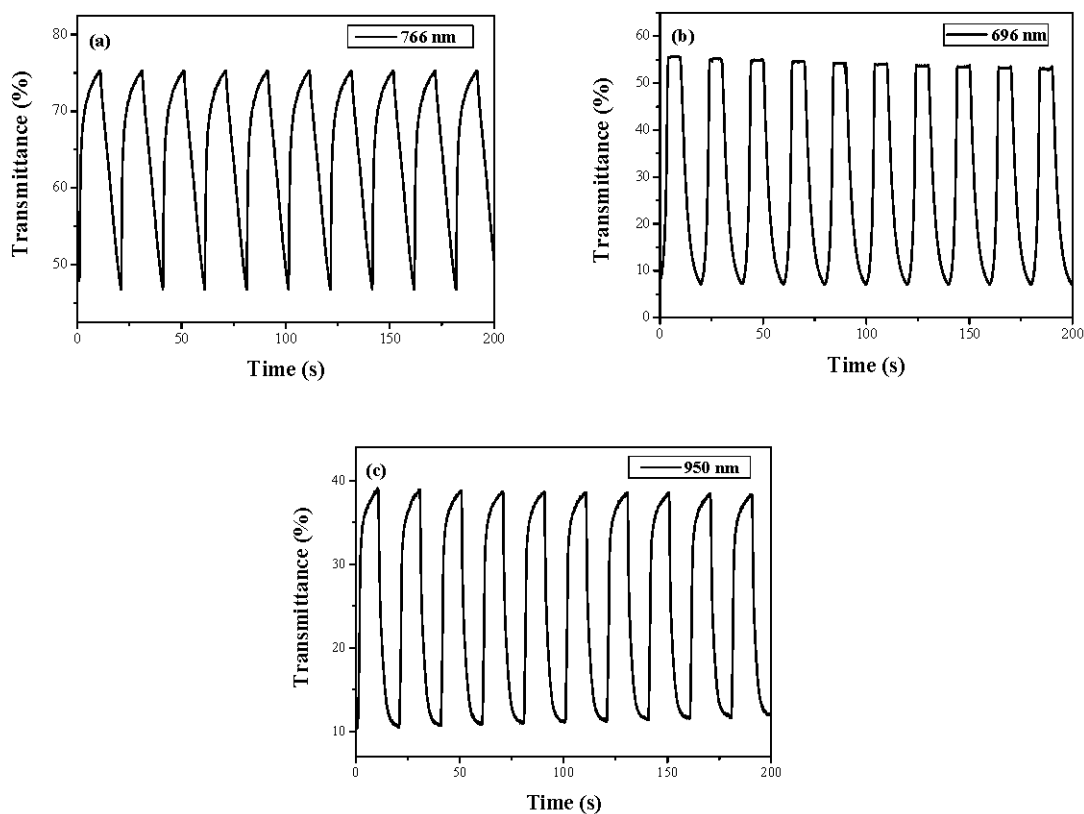
$$\Delta OD = \log \left( \frac{T_{\text{ox}}}{T_{\text{red}}} \right) \quad (1)$$

where  $T_{ox}$  and  $T_{red}$  represent the transmittance of the oxidized state and reduced state, respectively. The  $\Delta OD$  value of the PtnCz, P(tnCz1-bTp1), P(tnCz1-bTp2), P(tnCz1-bTp4), and PbTp films was 0.207, 0.766, 0.895, 0.652, and 0.559, respectively, in 0.2 M LiClO<sub>4</sub>/(ACN + DCM) solution. Similarly to the trend of  $\Delta T$ , the copolymers (P(tnCz1-bTp1), P(tnCz1-bTp2), and P(tnCz1-bTp4)) showed a higher  $\Delta OD$  value than the homopolymers (PtnCz and PbTp) in 0.2 M LiClO<sub>4</sub>/(ACN + DCM) solution.

The coloration efficiency ( $\eta$ ) can be calculated using the following equation:

$$\eta = \frac{\Delta OD}{Q_d} \quad (2)$$

where  $Q_d$  is the injected/ejected electronic charge of polymer films per active area and  $\Delta OD$  is the discrepancy of optical density. As listed in Table 3, the  $\eta$  value of the PtnCz film at 766 nm, the P(tnCz1-bTp1) film at 680 nm, the P(tnCz1-bTp2) film at 696 nm, the P(tnCz1-bTp4) film at 689 nm, and the PbTp film at 950 nm were 103.7, 180.3, 112.0, 150.1 and 83.5 cm<sup>2</sup>·C<sup>-1</sup>, respectively. The coloration response time ( $\tau_c$ ) and bleaching response time ( $\tau_b$ ) of the PtnCz, P(tnCz1-bTp1), P(tnCz1-bTp2), P(tnCz1-bTp4), and PbTp films in 0.2 M LiClO<sub>4</sub>/(ACN + DCM) solution are also shown in Table 3; the  $\tau_c$  and  $\tau_b$  values were calculated at 90% of the full-transmittance change.



**Figure 7.** Optical transmittance change of (a) PtnCz, (b) P(tnCz1-bTp2), and (c) PbTp electrodes in an ACN + DCM solution containing 0.2 M LiClO<sub>4</sub> with a residence time of 10 s.

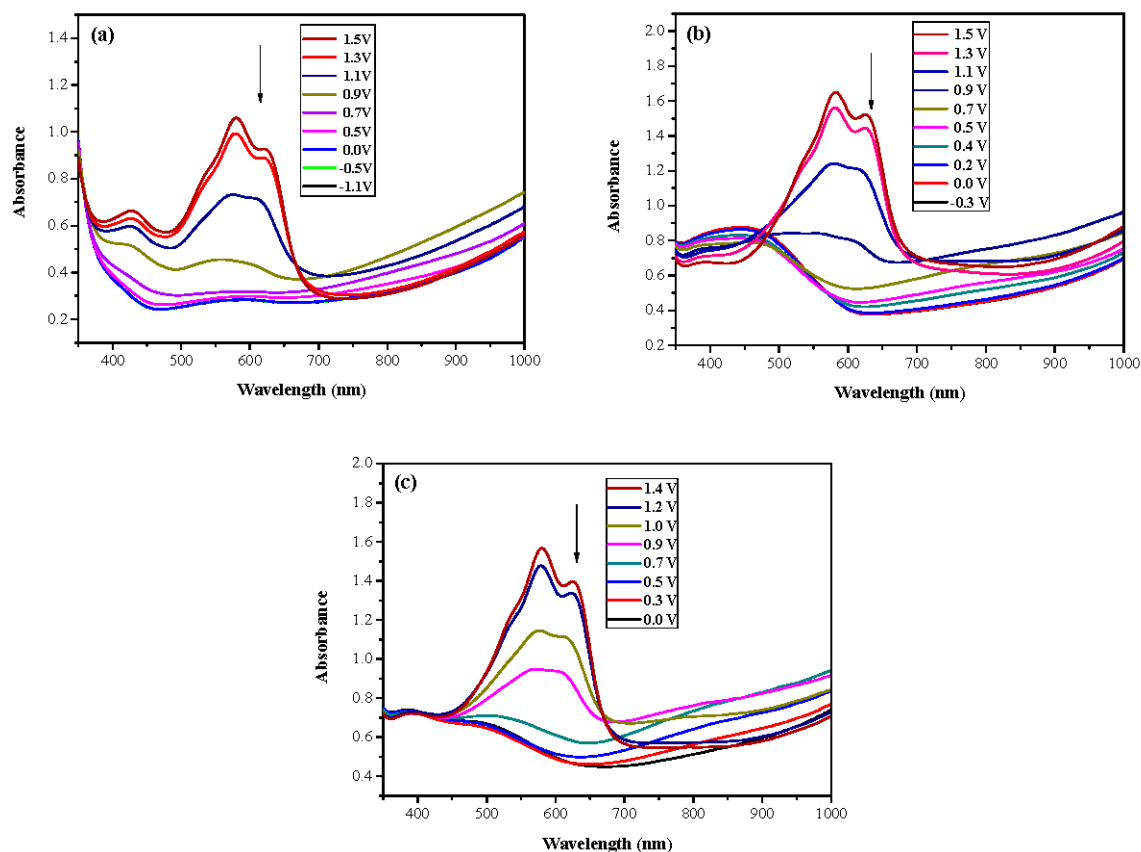
**Table 3.** Electrochromic characterizations of electrodes.

| Electrodes    | $\lambda$ (nm) | $T_{ox}$ (%) | $T_{red}$ (%) | $\Delta T$ (%) | Contrast (%) [23] | $\Delta OD$ | $Q_d$ (mC·cm <sup>-2</sup> ) | $\eta$ (cm <sup>2</sup> ·C <sup>-1</sup> ) | $\tau_c$ (s) | $\tau_b$ (s) |
|---------------|----------------|--------------|---------------|----------------|-------------------|-------------|------------------------------|--------------------------------------------|--------------|--------------|
| PtnCz         | 766            | 46.7         | 75.3          | 28.6           | 23.4              | 0.207       | 2.000                        | 103.7                                      | 5.5          | 4.5          |
| P(tnCz1-bTp1) | 680            | 9.3          | 54.3          | 45.0           | 70.8              | 0.766       | 4.250                        | 180.3                                      | 5.0          | 2.5          |
| P(tnCz1-bTp2) | 696            | 7.0          | 55.0          | 48.0           | 77.4              | 0.895       | 7.986                        | 112.0                                      | 6.0          | 4.0          |
| P(tnCz1-bTp4) | 689            | 10.5         | 47.2          | 36.7           | 63.6              | 0.652       | 4.346                        | 150.1                                      | 5.8          | 3.0          |
| PbTp          | 950            | 10.7         | 38.8          | 28.1           | 56.8              | 0.559       | 6.696                        | 83.5                                       | 5.5          | 4.5          |



### 3.3. Spectroelectrochemistry of ECDs

ECDs with the configurations of PtnCz/PProDOT-Me<sub>2</sub>, P(tnCz1-bTp1)/PProDOT-Me<sub>2</sub>, P(tnCz1-bTp2)/PProDOT-Me<sub>2</sub>, P(tnCz1-bTp4)/PProDOT-Me<sub>2</sub>, and PbTp/PProDOT-Me<sub>2</sub> were constructed. Figure 8a–c shows the UV-Vis spectra of PtnCz/PProDOT-Me<sub>2</sub>, P(tnCz1-bTp2)/PProDOT-Me<sub>2</sub>, and PbTp/PProDOT-Me<sub>2</sub> ECDs, respectively.



**Figure 8.** UV-Vis spectra of (a) PtnCz/PProDOT-Me<sub>2</sub>, (b) P(tnCz1-bTp2)/PProDOT-Me<sub>2</sub>, and (c) PbTp/PProDOT-Me<sub>2</sub> electrochromic devices (ECDs).

At 0.0 V, the PtnCz, P(tnCz1-bTp2), and PbTp films were in the neutral state, revealing light-grey, light-orange, and tangerine colors, respectively. The PProDOT-Me<sub>2</sub> film was in oxidized state, displaying a transparent blue color. Accordingly, the PtnCz/PProDOT-Me<sub>2</sub>, P(tnCz1-bTp2)/PProDOT-Me<sub>2</sub>, and PbTp/PProDOT-Me<sub>2</sub> ECDs did not show an obvious absorption peak below 400 nm. Upon increasing the potential gradually, the PtnCz, P(tnCz1-bTp2), and PbTp films began to oxidize, and the PProDOT-Me<sub>2</sub> film began to reduce. Therefore, new peaks at 580 and 630 nm emerged gradually, and the PtnCz/PProDOT-Me<sub>2</sub>, P(tnCz1-bTp2)/PProDOT-Me<sub>2</sub>, and PbTp/PProDOT-Me<sub>2</sub> ECDs revealed a dark blue color at 1.4–1.5 V. The electrochromic photographs, colorimetric values ( $L^*$ ,  $a^*$ , and  $b^*$ ), CIE chromaticity values ( $x$ ,  $y$ ) and CIE chromaticity diagrams of the PtnCz/PProDOT-Me<sub>2</sub> and P(tnCz1-bTp2)/PProDOT-Me<sub>2</sub> ECDs at various applied potentials are summarized in Table 4.

**Table 4.** Electrochromic photographs, colorimetric values ( $L^*$ ,  $a^*$ , and  $b^*$ ), CIE chromaticity values ( $x$ ,  $y$ ) and diagrams of the PtnCz/PProdot-Me<sub>2</sub> and P(tnCz1-bTp2)/PProdot-Me<sub>2</sub> electrochromic devices (ECDs) at various applied potentials.


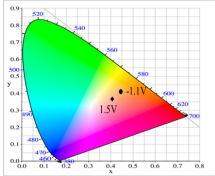





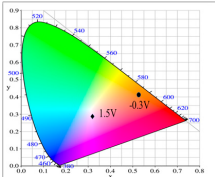




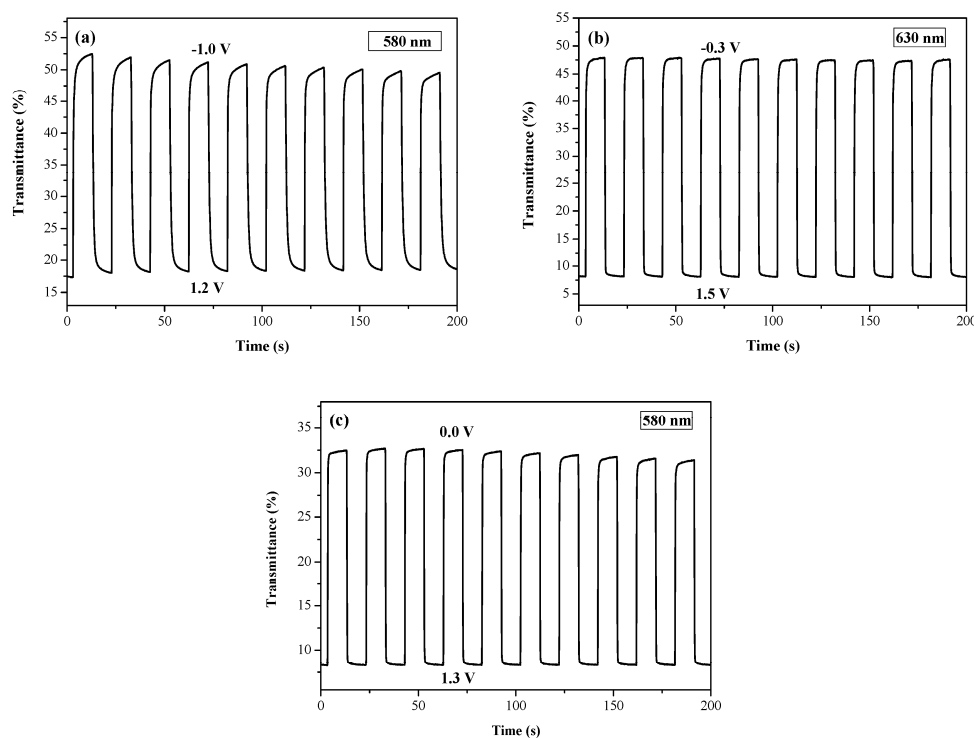
| ECDs                                      | Potential (V) | Photographs                                                                       | $L^*$ | $a^*$ | $b^*$  | $x$   | $y$   | Diagrams                                                                            |
|-------------------------------------------|---------------|-----------------------------------------------------------------------------------|-------|-------|--------|-------|-------|-------------------------------------------------------------------------------------|
| PtnCz/<br>PProdot-Me <sub>2</sub>         | −1.1          |  | 77.89 | −0.64 | −2.39  | 0.444 | 0.406 |  |
|                                           | 0.0           |  | 77.78 | −0.67 | −2.42  | 0.444 | 0.406 |                                                                                     |
|                                           | 0.9           |  | 67.00 | 2.70  | 1.82   | 0.456 | 0.406 |                                                                                     |
|                                           | 1.3           |  | 45.40 | 1.10  | −21.68 | 0.407 | 0.366 |                                                                                     |
|                                           | 1.5           |  | 43.60 | 1.45  | −22.35 | 0.405 | 0.362 |                                                                                     |
| P(tnCz1-bTp2)/<br>PProdot-Me <sub>2</sub> | −0.3          |  | 62.89 | 16.85 | 31.86  | 0.525 | 0.409 |  |
|                                           | 0.4           |  | 62.34 | 12.16 | 27.43  | 0.511 | 0.414 |                                                                                     |
|                                           | 0.7           |  | 58.41 | 6.68  | 18.02  | 0.489 | 0.416 |                                                                                     |
|                                           | 1.1           |  | 32.66 | 1.51  | −21.96 | 0.396 | 0.351 |                                                                                     |
|                                           | 1.5           |  | 25.34 | 0.30  | −41.33 | 0.318 | 0.284 |                                                                                     |

Figure 9 displays the transmittance profiles as a function of time for the PtnCz/PProDOT-Me<sub>2</sub>, P(tnCz1-bTp2)/PProDOT-Me<sub>2</sub>, and PbTp/PProDOT-Me<sub>2</sub> ECDs; the switching of the ECDs was monitored between −1.0 and 1.5 V with an interval of 10 s. The  $\Delta T$ ,  $\Delta OD$ ,  $\eta$ ,  $\tau_c$ , and  $\tau_b$  values of the PtnCz/PProDOT-Me<sub>2</sub>, P(tnCz1-bTp1)/PProDOT-Me<sub>2</sub>, P(tnCz1-bTp2)/PProDOT-Me<sub>2</sub>, P(tnCz1-bTp4)/PProDOT-Me<sub>2</sub>, and PbTp/PProDOT-Me<sub>2</sub> ECDs estimated at the 3rd and 50th cycles are shown in Table 5. The  $\Delta T$  value of the P(tnCz1-bTp1)/PProDOT-Me<sub>2</sub>, P(tnCz1-bTp2)/PProDOT-Me<sub>2</sub>, P(tnCz1-bTp4)/PProDOT-Me<sub>2</sub> ECDs was larger than that of the PbTp/PProDOT-Me<sub>2</sub> ECD, and the  $\Delta T$  value of the P(tnCz1-bTp1)/PProDOT-Me<sub>2</sub> and P(tnCz1-bTp2)/PProDOT-Me<sub>2</sub> ECDs showed a larger  $\Delta T$  value than that of the PtnCz/PProDOT-Me<sub>2</sub> ECD, indicating the incorporation of copolymers as the anodic layers gave rise to a higher  $\Delta T$  than those of the homopolymers (PtnCz and PbTp). The  $\Delta T$  value of the PtnCz/PProDOT-Me<sub>2</sub>, P(tnCz1-bTp1)/PProDOT-Me<sub>2</sub>, P(tnCz1-bTp2)/PProDOT-Me<sub>2</sub>, P(tnCz1-bTp4)/PProDOT-Me<sub>2</sub>, and PbTp/PProDOT-Me<sub>2</sub> ECDs was greater than that of the PtnCz, P(tnCz1-bTp1), P(tnCz1-bTp2), P(tnCz1-bTp4) and PbTp films, respectively, in 0.2 M LiClO<sub>4</sub>/(ACN + DCM) solution; this could be accredited to ECDs containing anodic and cathodic layers but there being no complementary electrode for PtnCz, P(tnCz1-bTp1), P(tnCz1-bTp2), P(tnCz1-bTp4) and PbTp films in a solution. The  $\tau_b$  and  $\tau_c$  values of the PtnCz/PProDOT-Me<sub>2</sub>, P(tnCz1-bTp1)/PProDOT-Me<sub>2</sub>, P(tnCz1-bTp2)/PProDOT-Me<sub>2</sub>, P(tnCz1-bTp4)/PProDOT-Me<sub>2</sub>, and PbTp/PProDOT-Me<sub>2</sub> ECDs were smaller than those of the PtnCz, P(tnCz1-bTp1), P(tnCz1-bTp2), P(tnCz1-bTp4), and PbTp films, respectively, in 0.2 M LiClO<sub>4</sub>/(ACN + DCM) solution, implying that the ECDs changed color faster from the bleached to the colored states and from the colored to the bleached states than did the PtnCz, P(tnCz1-bTp1), P(tnCz1-bTp2), P(tnCz1-bTp4), and PbTp films in 0.2 M LiClO<sub>4</sub>/(ACN + DCM) solution.



**Figure 9.** Optical transmittance change of (a) PtnCz/PProDOT-Me<sub>2</sub>, (b) P(tnCz1-bTp2)/PProDOT-Me<sub>2</sub>, and (c) PbTp/PProDOT-Me<sub>2</sub> electrochromic devices (ECDs) with a residence time of 10 s.

**Table 5.** Electrochromic characterizations of electrochromic devices (ECDs).

| ECDs                                                        | N  | T <sub>ox</sub> (%) | T <sub>red</sub> (%) | ΔT (%) | Contrast (%) | ΔOD   | Q <sub>d</sub> (mC·cm <sup>-2</sup> ) | η (cm <sup>2</sup> ·C <sup>-1</sup> ) | τ <sub>c</sub> (s) | τ <sub>b</sub> (s) |
|-------------------------------------------------------------|----|---------------------|----------------------|--------|--------------|-------|---------------------------------------|---------------------------------------|--------------------|--------------------|
| PtnCz/PProdot-Me <sub>2</sub> (580 nm) <sup>a</sup>         | 3  | 18.2                | 51.4                 | 33.2   | 47.7         | 0.450 | 0.859                                 | 523.9                                 | 2.5                | 0.5                |
|                                                             | 50 | 19.5                | 44.0                 | 24.5   | 38.6         | 0.353 | 0.620                                 | 569.4                                 | 1.0                | 1.0                |
| P(tnCz1-bTp1)/PProdot-Me <sub>2</sub> (582 nm) <sup>a</sup> | 3  | 7.1                 | 42.1                 | 35.0   | 71.1         | 0.773 | 1.596                                 | 484.3                                 | 0.5                | 0.5                |
|                                                             | 50 | 7.5                 | 39.0                 | 31.5   | 67.7         | 0.716 | 1.252                                 | 571.8                                 | 2.0                | 2.0                |
| P(tnCz1-bTp2)/PProdot-Me <sub>2</sub> (630 nm) <sup>a</sup> | 3  | 8.0                 | 48.0                 | 40.0   | 71.4         | 0.778 | 1.500                                 | 518.8                                 | 0.8                | 0.3                |
|                                                             | 50 | 7.4                 | 46.0                 | 38.6   | 72.3         | 0.793 | 1.470                                 | 539.4                                 | 0.7                | 0.5                |
| P(tnCz1-bTp4)/PProdot-Me <sub>2</sub> (624 nm) <sup>a</sup> | 3  | 11.5                | 39.2                 | 27.7   | 54.6         | 0.532 | 0.953                                 | 558.7                                 | 0.5                | 0.5                |
|                                                             | 50 | 9.6                 | 32.3                 | 22.7   | 54.2         | 0.526 | 0.981                                 | 537.1                                 | 0.5                | 0.7                |
| PbTp/PProdot-Me <sub>2</sub> (580 nm) <sup>a</sup>          | 3  | 8.2                 | 32.6                 | 24.4   | 59.8         | 0.599 | 1.106                                 | 541.6                                 | 0.5                | 0.5                |
|                                                             | 50 | 8.3                 | 28.9                 | 20.6   | 55.4         | 0.542 | 0.908                                 | 596.6                                 | 0.5                | 0.5                |

<sup>a</sup> The selected applied wavelength for the ECDs.

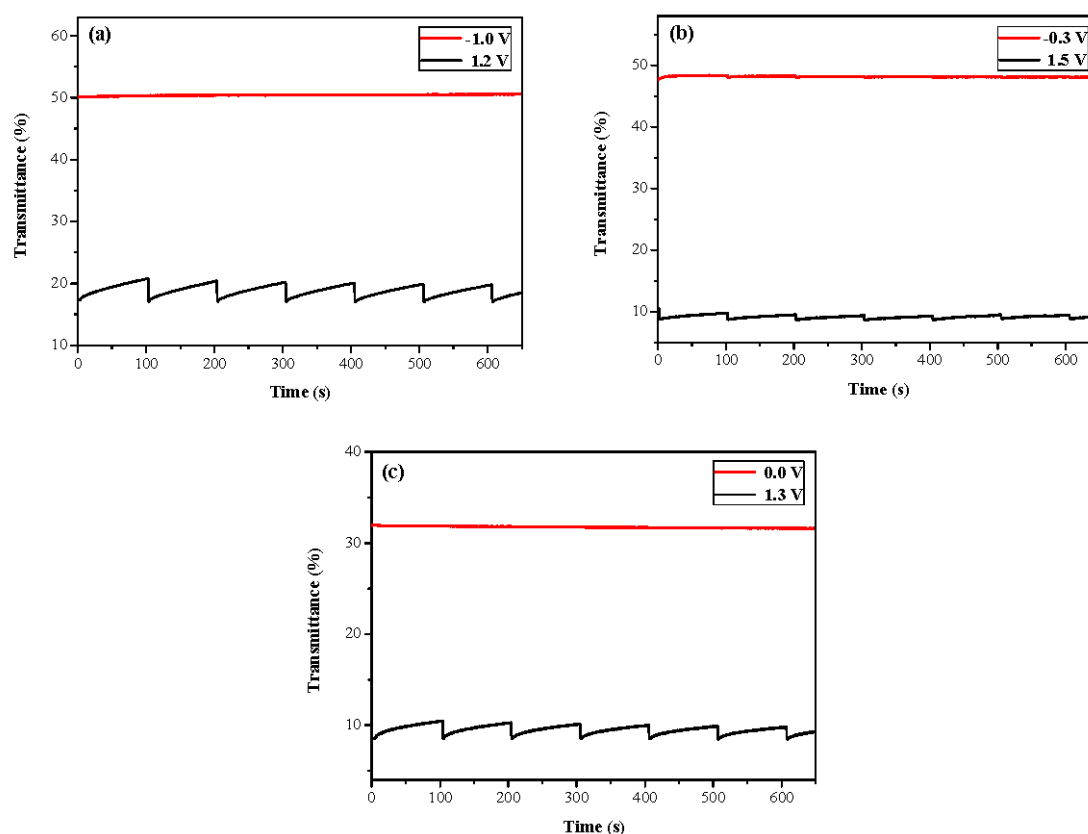
The comparisons of  $\Delta T_{\max}$  and  $\eta$  for the reported ECDs are summarized in Table 6; the P(tnCz1-bTp2)/PProDOT-Me<sub>2</sub> ECD showed a higher  $\Delta T_{\max}$  than that reported for the PdNCz/PEDOT [36], PbmCz/PEDOT [37], PHCz/PEDOT [38], P(dNCz-Hcp)/PEDOT [39], P(dNCz-bT)/PEDOT [40], and P(Cz4-6CIn1)/PProDOT-Me<sub>2</sub> ECDs [41], and the  $\Delta T_{\max}$  value of the P(tnCz1-bTp2)/PProDOT-Me<sub>2</sub> ECD as comparable to that of the P(BCz-ProDOTme)/PEDOT-PSS ECD [42]. In addition, the  $\Delta T$  value of the P(tnCz1-bTp2) ECD was lower than that reported for a non-mechanical microiris based on viologen and phenazine complementary electrochromic materials [43]. On the other hand, the P(tnCz1-bTp2)/PProDOT-Me<sub>2</sub> ECD showed a higher  $\eta$  value at 630 nm than was reported for the PHCz/PEDOT [38], P(dNCz-Hcp)/PEDOT [39], P(dNCz-bT)/PEDOT [40], P(Cz4-6CIn1)/PProDOT-Me<sub>2</sub> [41], and P(BCz-ProDOTme)/PEDOT-PSS ECDs [42]. The high  $\Delta T_{\max}$  and  $\eta$  values of the P(tnCz1-bTp2)/PProDOT-Me<sub>2</sub> ECD makes P(tnCz1-bTp2) a potential electrochromic material for ECD applications.

**Table 6.** Coloration efficiencies and transmission changes of electrochromic devices (ECDs).

| ECD Configuration                     | $\Delta T_{\max}$ (%) | $\eta_{\max}$ (cm <sup>2</sup> ·C <sup>-1</sup> ) | Reference |
|---------------------------------------|-----------------------|---------------------------------------------------|-----------|
| PdNCz/PEDOT                           | 19 (550 nm)           | —                                                 | [36]      |
| PbmCz/PEDOT                           | 35 (620 nm)           | —                                                 | [37]      |
| PHCz/PEDOT                            | 23 (623 nm)           | 290                                               | [38]      |
| P(dNCz-Hcp)/PEDOT                     | 39.8 (628 nm)         | 319.98                                            | [39]      |
| P(dNCz-bT)/PEDOT                      | 28.6 (700 nm)         | 234                                               | [40]      |
| P(Cz4-6CIn1)/PProDOT-Me <sub>2</sub>  | 32 (575 nm)           | 372.7                                             | [41]      |
| P(BCz-ProDOTme)/PEDOT-PSS             | 41 (642 nm)           | 417                                               | [42]      |
| P(tnCz1-bTp2)/PProdot-Me <sub>2</sub> | 40 (630 nm)           | 539                                               | This work |

### 3.4. Open Circuit Memory of Electrochromic Devices

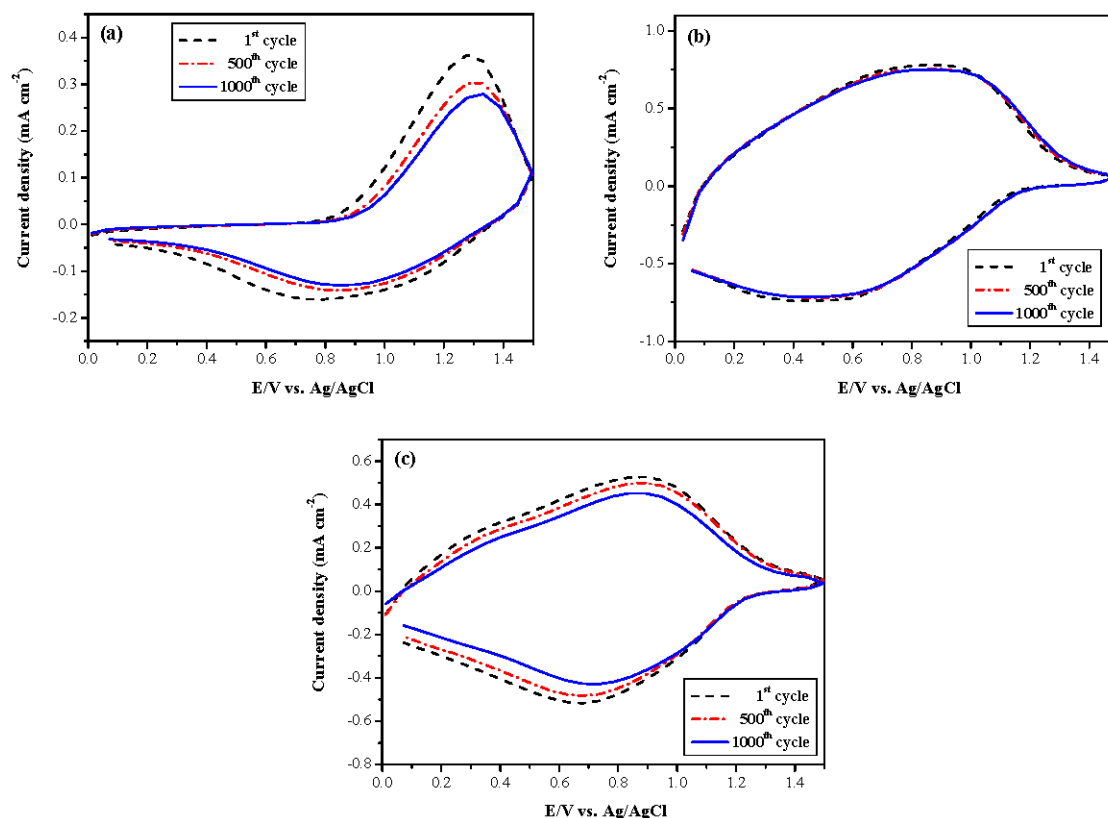
The ability to maintain bleached and colored states in the open circuit of the PtnCz/PProDOT-Me<sub>2</sub>, P(tnCZ1-bTp2)/PProDOT-Me<sub>2</sub>, and PbTp/PProDOT-Me<sub>2</sub> ECDs was monitored at a specific wavelength as a function of the time in the bleached and colored states by applying the voltage for 1 s for each 200 s time interval. As shown in Figure 10, the P(tnCZ1-bTp2)/PProDOT-Me<sub>2</sub> ECD showed good optical memories in the neutral state of the P(tnCZ1-bTp2) film; almost no transmittance change in the neutral state was observed. In the oxidation state of the P(tnCZ1-bTp2) film, the P(tnCZ1-bTp2)/PProDOT-Me<sub>2</sub> ECD was rather less stable than the P(tnCZ1-bTp2) film in the neutral state, but the transmittance change was less than 3% in the oxidation state of the P(tnCZ1-bTp2) film, implying that the P(tnCZ1-bTp2)/PProDOT-Me<sub>2</sub> ECD showed a reasonable open-circuit memory.



**Figure 10.** Optical memory of the (a) PtnCz/PProDOT-Me<sub>2</sub>, (b) P(tnCZ1-bTp2)/PProDOT-Me<sub>2</sub>, and (c) PbTp/PProDOT-Me<sub>2</sub> electrochromic devices (ECDs).

### 3.5. Switching Stability of Electrochromic Devices

The switching stability of the PtnCz/PProDOT-Me<sub>2</sub>, P(tnCz1-bTp2)/PProDOT-Me<sub>2</sub>, and PbTp/PProDOT-Me<sub>2</sub> ECDs for multiple cycles was measured using CV at voltages between 0.0 and 1.5 V. As displayed in Figure 11, 81.7%, 99.7%, and 92.4% electroactivity was retained after 500 cycles for the PtnCz/PProDOT-Me<sub>2</sub>, P(tnCz1-bTp2)/PProDOT-Me<sub>2</sub>, and PbTp/PProDOT-Me<sub>2</sub> ECDs, respectively, and 73.3%, 99.3%, and 81.4% electroactivity was retained after 1000 cycles for the PtnCz/PProDOT-Me<sub>2</sub>, P(tnCz1-bTp2)/PProDOT-Me<sub>2</sub>, and PbTp/PProDOT-Me<sub>2</sub> ECDs, respectively. The P(tnCz1-bTp2)/PProDOT-Me<sub>2</sub> ECD employing the P(tnCz1-bTp2) copolymer as an anodic polymer layer shows better multiple switching stability than the homopolymers as anodic layers for the PtnCz/PProDOT-Me<sub>2</sub> and PbTp/PProDOT-Me<sub>2</sub> ECDs.



**Figure 11.** CVs of (a) PtnCz/PProDOT-Me<sub>2</sub>, (b) P(tnCz1-bTp2)/PProDOT-Me<sub>2</sub>, and (c) PbTp/PProDOT-Me<sub>2</sub> electrochromic devices (ECDs) with a scan rate of 500 mV·s<sup>-1</sup> between 1st and 1000th cycles.

## 4. Conclusions

Two anodic homopolymer films (PtnCz and PbTp) and three anodic copolymer films (P(tnCz1-bTp1), P(tnCz1-bTp2), and P(tnCz1-bTp4)) were prepared using electrochemical polymerization. The electrochromic studies of anodic polymer films in 0.2 M LiClO<sub>4</sub>/(ACN + DCM) solution exhibited that the P(tnCz1-bTp2) film was light-orange in the neutral state, yellowish-orange in the intermediate state, yellowish-green in the oxidized state, and blue in highly oxidized states. Electrochromic switching characterizations of anodic polymer films in 0.2 M LiClO<sub>4</sub>/(ACN + DCM) solution showed high  $\Delta T_{\max}$  values for P(tnCz1-bTp2) (48% at 696 nm) and P(tnCz1-bTp1) (45% at 680 nm). The electrochromic behaviors of five ECDs (PtnCz/PProDOT-Me<sub>2</sub>, P(tnCz1-bTp1)/PProDOT-Me<sub>2</sub>, P(tnCz1-bTp2)/PProDOT-Me<sub>2</sub>, P(tnCz1-bTp4)/PProDOT-Me<sub>2</sub>, and PbTp/PProDOT-Me<sub>2</sub> ECDs) were characterized. The P(tnCz1-bTp2)/PProDOT-Me<sub>2</sub> ECD revealed a high  $\Delta T_{\max}$  value

(40% at 630 nm), a high  $\eta$  value ( $539.4 \text{ cm}^2 \cdot \text{C}^{-1}$  at 630 nm), a satisfactory open-circuit memory, and a satisfactory redox cycling stability. On the basis of the above results, the P(tnCz1-bTp2)/PProDOT-Me<sub>2</sub> ECD is a candidate for applications in self-dimming mirrors and energy-saving windows.

**Acknowledgments:** The authors would like to thank the Ministry of Science and Technology (MOST) of the Republic of China for financially supporting this project.

**Author Contributions:** Chung-Wen Kuo designed and conceived the experiments, analyzed the data, and wrote the paper; Po-Ying Lee implemented partial experiments.

**Conflicts of Interest:** The authors declare no conflict of interest.

## References

1. Zhang, S.; Li, X.; Chu, D. An organic electroactive material for flow batteries. *Electrochim. Acta* **2016**, *190*, 737–743. [[CrossRef](#)]
2. Hsiao, S.H.; Wu, C.N. Electrochemical and electrochromic studies of redox-active aromatic polyamides with 3,5-dimethyltriphenylamine units. *J. Electroanal. Chem.* **2016**, *776*, 139–147. [[CrossRef](#)]
3. Zhu, Z.; Chen, J. Review-advanced carbon-supported organic electrode materials for lithium (sodium)-ion batteries. *J. Electrochem. Soc.* **2015**, *162*, A2393–A2405. [[CrossRef](#)]
4. Kerszulis, J.A.; Johnson, K.E.; Kuepfert, M.; Khoshabo, D.; Dyerac, A.L.; Reynolds, J.R. Tuning the painter's palette: Subtle steric effects on spectra and colour in conjugated electrochromic polymers. *J. Mater. Chem. C* **2015**, *3*, 3211–3218. [[CrossRef](#)]
5. Chou, J.C.; Huang, Y.C.; Wu, T.Y.; Liao, Y.H.; Lai, C.H.; Chu, C.M.; Lin, Y.J. Poly(3,3-dibenzyl-3,4-dihydro-2H-thieno[3,4-b][1,4]dioxepine)/platinum composite films as potential counter electrodes for dye-sensitized solar cells. *Polymers* **2017**, *9*, 271. [[CrossRef](#)]
6. Che Balian, S.R.; Ahmad, A.; Mohamed, N.S. The effect of lithium iodide to the properties of carboxymethyl  $\kappa$ -carrageenan/carboxymethyl cellulose polymer electrolyte and dye-sensitized solar cell performance. *Polymers* **2016**, *8*, 163. [[CrossRef](#)]
7. Selvaraj, V.; Alagar, M.; Hamerton, I. Electrocatalytic properties of monometallic and bimetallic nanoparticles-incorporated polypyrrole films for electro-oxidation of methanol. *J. Power Sources* **2006**, *160*, 940–948. [[CrossRef](#)]
8. Wu, T.Y.; Chen, B.K.; Chang, J.K.; Chen, P.R.; Kuo, C.W. Nanostructured poly(aniline-co-metaniic acid) as platinum catalyst support for electro-oxidation of methanol. *Int. J. Hydrog. Energy* **2015**, *40*, 2631–2640. [[CrossRef](#)]
9. Nagashree, K.L.; Raviraj, N.H.; Ahmed, M.F. Carbon paste electrodes modified by Pt and Pt-Ni microparticles dispersed in polyindole film for electrocatalytic oxidation of methanol. *Electrochim. Acta* **2010**, *55*, 2629–2635. [[CrossRef](#)]
10. Hsieh, S.N.; Hsiao, S.W.; Chen, T.Y.; Li, C.Y.; Lee, C.H.; Guo, T.F.; Hsu, Y.J.; Lin, T.L.; Wei, Y.; Wen, T.C. Self-assembled tetraoctylammonium bromide as an electron-injection layer for cathode-independent high-efficiency polymer light-emitting diodes. *J. Mater. Chem.* **2011**, *21*, 8715–8720. [[CrossRef](#)]
11. Al-Asbahi, B.A.; Haji Jumali, M.H.; AlSalhi, M.S. Enhanced optoelectronic properties of PFO/fluorol 7GA hybrid light emitting diodes via additions of TiO<sub>2</sub> nanoparticles. *Polymers* **2016**, *8*, 334. [[CrossRef](#)]
12. Hsieh, S.N.; Chen, S.P.; Li, C.Y.; Wen, T.C.; Guo, T.F.; Hsu, Y.J. Surface modification of TiO<sub>2</sub> by a self-assembly monolayer in inverted-type polymer light-emitting devices. *Org. Electron.* **2009**, *10*, 1626–1631. [[CrossRef](#)]
13. Iro, Z.S.; Subramani, C.; Dash, S.S. A brief review on electrode materials for supercapacitor. *Int. J. Electrochem. Sci.* **2016**, *11*, 10628–10643. [[CrossRef](#)]
14. Fu, W.C.; Hsieh, Y.T.; Wu, T.Y.; Sun, I.W. Electrochemical preparation of porous poly(3,4-ethylenedioxythiophene) electrodes from room temperature ionic liquids for supercapacitors. *J. Electrochem. Soc.* **2016**, *163*, G61–G68. [[CrossRef](#)]
15. Wu, T.Y.; Sheu, R.B.; Chen, Y. Synthesis and optically acid-sensory and electrochemical properties of novel polyoxadiazole derivatives. *Macromolecules* **2004**, *37*, 725–733. [[CrossRef](#)]
16. Hung, C.C.; Wen, T.C.; Wei, Y. Site-selective deposition of ultra-fine Au nanoparticles on polyaniline nanofibers for H<sub>2</sub>O<sub>2</sub> sensing. *Mater. Chem. Phys.* **2010**, *122*, 392–396. [[CrossRef](#)]

17. Chang, K.H.; Wang, H.P.; Wu, T.Y.; Sun, I.W. Optical and electrochromic characterizations of four 2,5-dithienylpyrrole-based conducting polymer films. *Electrochim. Acta* **2014**, *119*, 225–235. [[CrossRef](#)]
18. Cansu-Ergun, E.G.; Onal, A.M.; Cihaner, A. Propylenedioxy and benzimidazole based electrochromic polymers. *J. Electrochem. Soc.* **2016**, *163*, G53–G60. [[CrossRef](#)]
19. Wu, T.Y.; Li, W.B.; Kuo, C.W.; Chou, C.F.; Liao, J.W.; Chen, H.R.; Tseng, C.G. Study of poly(methyl methacrylate)-based gel electrolyte for electrochromic device. *Int. J. Electrochem. Sci.* **2013**, *8*, 10720–10732.
20. Gadgil, B.; Damlin, P.; Dmitrieva, E.; Ääritalo, T.; Kvarnström, C. ESR/UV-Vis-NIR spectroelectrochemical study and electrochromic contrast enhancement of a polythiophene derivative bearing a pendant viologen. *RSC Adv.* **2015**, *5*, 42242–42249. [[CrossRef](#)]
21. Schottland, P.; Zong, K.; Gaupp, C.L.; Thompson, B.C.; Thomas, C.A.; Giurgiu, I.; Hickman, R.; Abboud, K.A.; Reynolds, J.R. Poly(3,4-alkylenedioxythiophene)s: Highly stable electronically conducting and electrochromic polymers. *Macromolecules* **2000**, *33*, 7051–7061. [[CrossRef](#)]
22. Deutschmann, T.; Oesterschulze, E. Integrated electrochromic iris device for low power and space-limited applications. *J. Opt.* **2014**, *16*. [[CrossRef](#)]
23. Deutschmann, T.; Oesterschulze, E. Micro-structured electrochromic device based on poly(3,4-ethylenedioxythiophene). *J. Micromech. Microeng.* **2013**, *23*. [[CrossRef](#)]
24. Roth, S.; Ignatowitz, M.; Muller, P.; Monch, W.; Oesterschulze, E. Non-mechanical variable apertures based on poly(3,4-ethylenedioxythiophene) (PEDOT). *Microelectron. Eng.* **2011**, *88*, 2349–2351. [[CrossRef](#)]
25. Hsiao, S.H.; Hsueh, J.C. Electrochemical synthesis and electrochromic properties of new conjugated polycarbazoles from di(carbazol-9-yl)-substituted triphenylamine and *N*-phenylcarbazole derivatives. *J. Electroanal. Chem.* **2015**, *758*, 100–110. [[CrossRef](#)]
26. Kuo, C.W.; Wu, T.Y.; Huang, M.W. Electrochromic characterizations of copolymers based on 4,4'-bis(*N*-carbazolyl)-1,1'-biphenyl and indole-6-carboxylic acid and their applications in electrochromic devices. *J. Taiwan Inst. Chem. Eng.* **2016**, *68*, 481–488. [[CrossRef](#)]
27. Soyleyici, S.; Karakus, M.; Ak, M. Transparent-blue colored dual type electrochromic device: Switchable glass application of conducting organic-inorganic hybrid carbazole polymer. *J. Electrochem. Soc.* **2016**, *163*, H679–H683. [[CrossRef](#)]
28. Wu, T.Y.; Tsai, C.J.; Tseng, L.Y.; Chen, S.J.; Hsieh, T.H.; Kuo, C.W. Nanocomposite of platinum particles embedded into nanosheets of polycarbazole for methanol oxidation. *J. Chin. Chem. Soc.* **2014**, *61*, 860–866. [[CrossRef](#)]
29. Hsiao, S.H.; Lin, S.W. Electrochemical synthesis of electrochromic polycarbazole films from *N*-phenyl-3,6-bis(*N*-carbazolyl)carbazoles. *Polym. Chem.* **2016**, *7*, 198–211. [[CrossRef](#)]
30. Zhang, Y.; Liu, X.; Wang, M.; Liu, X.; Zhao, J. Low band gap donor–acceptor type polymers containing 2,3-bis(4-(decyloxy)phenyl)pyrido[4,3-*b*]pyrazine as acceptor and different thiophene derivatives as donors. *Polymers* **2016**, *8*, 377. [[CrossRef](#)]
31. Welsh, D.M.; Kumar, A.; Meijer, E.W.; Reynolds, J.R. Enhanced contrast ratio and rapid switching in electrochromics based on poly(3,4-propylenedioxythiophene) derivatives. *Adv. Mater.* **1999**, *11*, 1379–1382. [[CrossRef](#)]
32. Kuo, C.W.; Chen, B.K.; Li, W.B.; Tseng, L.Y.; Wu, T.Y.; Tseng, C.G.; Chen, H.R.; Huang, Y.C. Effects of supporting electrolytes on spectroelectrochemical and electrochromic properties of polyaniline-poly(styrene sulfonic acid) and poly(ethylenedioxythiophene)-poly(styrene sulfonic acid)-based electrochromic device. *J. Chin. Chem. Soc.* **2014**, *61*, 563–570. [[CrossRef](#)]
33. Yigitsoy, B.; Varis, S.; Tanyeli, C.; Akhmedov, I.M.; Toppare, L. Electrochromic properties of a novel low band gap conductive copolymer. *Electrochim. Acta* **2007**, *52*, 6561–6568. [[CrossRef](#)]
34. Hsiao, S.H.; Wu, L.C. Fluorescent and electrochromic polymers from 2,8-di(carbazol-9-yl)dibenzothiophene and its *S*, *S*-dioxide derivative. *Dyes Pigments* **2016**, *134*, 51–63. [[CrossRef](#)]
35. Wu, T.Y.; Chung, H.H. Applications of tris(4-(thiophen-2-yl)phenyl)amine- and dithienylpyrrole-based conjugated copolymers in high-contrast electrochromic devices. *Polymers* **2016**, *8*, 206. [[CrossRef](#)]
36. Koyuncu, S.; Gultekin, B.; Zafer, C.; Bilgili, H.; Can, M.; Demic, S.; Kaya, I.; Icli, S. Electrochemical and optical properties of biphenyl bridged-dicarbazole oligomer films: Electropolymerization and electrochromism. *Electrochim. Acta* **2009**, *54*, 5694–5702. [[CrossRef](#)]

37. Udum, Y.A.; Gündoğdu Hızlıates, C.; Ergün, Y.; Toppare, L. Electrosynthesis and characterization of an electrochromic material containing biscarbazole-oxadiazole units and its application in an electrochromic device. *Thin Solid Films* **2015**, *595*, 61–67. [[CrossRef](#)]
38. Wang, B.; Zhao, J.; Xiao, J.; Cui, C.; Liu, R. Synthesis and electropolymerization of 9H-carbazol-9-ylpyrene and its electrochromic properties and electrochromic device application. *Int. J. Electrochem. Sci.* **2012**, *7*, 2781–2795.
39. Chen, S.; Gao, Q.; Zhao, J.; Cui, C.; Yang, W.; Zhang, X. Electrosyntheses, characterizations and electrochromic properties of a novel copolymer of 4,4'-di(*N*-carbazoyl)biphenyl with 4H-cyclopenta[2,1-b:3,4-b']dithiophene. *Int. J. Electrochem. Sci.* **2012**, *7*, 5256–5272.
40. Wang, B.; Zhao, J.; Liu, R.; Liu, J.; He, Q. Electrosyntheses, characterizations and electrochromic properties of a copolymer based on 4,4'-di(*N*-carbazoyl)biphenyl and 2,2'-bithiophene. *Sol. Energy Mater. Sol. Cells* **2011**, *95*, 1867–1874. [[CrossRef](#)]
41. Kuo, C.W.; Hsieh, T.H.; Hsieh, C.K.; Liao, J.W.; Wu, T.Y. Electrosynthesis and characterization of four electrochromic polymers based on carbazole and indole-6-carboxylic acid and their applications in high-contrast electrochromic devices. *J. Electrochem. Soc.* **2014**, *161*, D782–D790. [[CrossRef](#)]
42. Kuo, C.W.; Wu, T.L.; Lin, Y.C.; Chang, J.K.; Chen, H.R.; Wu, T.Y. Copolymers based on 1,3-bis(carbazol-9-yl)benzene and three 3,4-ethylenedioxythiophene derivatives as potential anodically coloring copolymers in high-contrast electrochromic devices. *Polymers* **2016**, *8*, 368. [[CrossRef](#)]
43. Deutschmann, T.; Kortz, C.; Walder, L.; Oesterschulze, E. High contrast electrochromic iris. *Opt. Express* **2015**, *23*, 31544–31549. [[CrossRef](#)] [[PubMed](#)]



© 2017 by the authors. Licensee MDPI, Basel, Switzerland. This article is an open access article distributed under the terms and conditions of the Creative Commons Attribution (CC BY) license (<http://creativecommons.org/licenses/by/4.0/>).